Second International Conference on CFD in the Minerals and Process Industries
CSIRO, Melbourne, Australia
6-8 December 1999

APPLICATION OF THE REVISED WILCOX (1998) k- ω TURBULENCE MODEL TO A JET IN CO-FLOW

R. C. MORGANS[1], B. B. DALLY[1], G. J. NATHAN[1], P. V. LANSPEARY[1] and D. F. FLETCHER[2]

[1] Department of Mechanical Engineering, University of Adelaide, South Australia 5005, AUSTRALIA
[2] Department of Chemical Engineering, University of Sydney, New South Wales 2006, AUSTRALIA

ABSTRACT

The performance of the Wilcox (1998) k-ω turbulence model is compared with the standard k-ε model, and with a modified k-ε model in an elliptic flow solver. The flow selected for this comparison is a round jet issuing from a pipe and surrounded by a co-flow, but without the influence of confinement (Schefer, Hartmann and Dibble, 1987). This is a necessary test prior to studying more complex flows.

The Wilcox (1998) k-ω model gives a prediction of the round-jet spreading rate similar to that of the modified k-ε model and better than that of the standard k-ε model. However with the current implementation of the k-ω model, the convergence of the solution is sensitive to the choice of boundary location and to the boundary values of k and ω. This sensitivity is currently under investigation.

NOMENCLATURE

$C_{\varepsilon 1}$	Dissipation rate equation production coefficient
$C_{\varepsilon 2}$	Dissipation rate equation dissipation coefficient
C_μ	Eddy viscosity coefficient
D_j	Internal pipe diameter
f_β	Bounded vortex stretching function ($7/8 \le f_\beta \le 1$)
f_{β^*}	Bounded cross diffusion function ($1 \le f_{\beta^*} \le 1.7$)
k	Kinetic energy of turbulent fluctuation per unit mass
r	Radial distance
$r_{1/2}$	Half width (Radius at which velocity is half the centreline value)
R	Pipe radius ($D_j/2$)
Re_{pipe}	Pipe Reynolds number ($D_j U_{cl}/\nu$)
R_T	Turbulence Reynolds number
S_{ij}	Mean strain rate tensor, $S_{ij} = \frac{1}{2}\left(\frac{\partial U_i}{\partial x_j} + \frac{\partial U_j}{\partial x_i}\right)$
u'	Axial velocity fluctuations
U_{bulk}	Bulk Velocity
U_{cl}	Centreline velocity
U_{co}	Co-flow velocity
$U_{e,cl}$	Centreline exit velocity
U_j	Mean velocity
U_τ	Friction velocity, $U_\tau = \sqrt{\frac{\tau_w}{\rho}}$
v'	Radial velocity fluctuations
w'	Radial velocity fluctuations
y	Distance from wall
y^+	Dimensionless distance from the wall, based on sublayer parameters, $y^+ = \frac{yU_\tau}{\nu}$
α	Production coefficient for specific dissipation rate (Wilcox model)
β^*	Dissipation rate coefficient for turbulence kinetic energy (Wilcox model)
β	Dissipation coefficient for specific dissipation rate (Wilcox model)
δ	Boundary layer thickness
δ_{ij}	Kronecker delta
ε	Modelled dissipation rate per unit mass
μ	Dynamic molecular viscosity
ν	Kinematic molecular viscosity (μ/ρ)
ν_T	Kinematic eddy viscosity
ρ	Density
σ^*	Reciprocal of turbulent Prandtl number for kinetic energy (Wilcox model)
σ	Reciprocal of turbulent Prandtl number for specific dissipation rate (Wilcox model)
σ_k	Turbulent Prandtl number for kinetic energy (k-ε model)
σ_ε	Turbulent Prandtl number for dissipation rate (k-ε model)
τ_{ij}	Specific Reynolds stress tensor ($-\overline{u_i' u_j'}$)
τ_w	Wall shear stress
χ_k	Cross diffusion parameter
χ_ω	Vortex-stretching parameter
ω	Specific dissipation rate
Ω_{ij}	Mean rotation tensor, $\Omega_{ij} = \frac{1}{2}\left(\frac{\partial U_i}{\partial x_j} - \frac{\partial U_j}{\partial x_i}\right)$

INTRODUCTION

Industrial flows usually contain complex arrangements of boundary-layers and free-shear flows. Turbulent jets are widely used for mixing two streams of fluid, as for example, in combustion where a fuel jet flow is commonly injected into a co-flowing stream of air.

To predict industrial flows, it is therefore highly desirable for a single turbulence model to be capable of simulating both boundary-layers and free-shear flows without requiring prior knowledge of their location within the computational domain.

Without viscous corrections the widely used standard k-ε turbulence model fails to predict flow near a solid boundary. It also fails to predict the experimentally observed difference between the spreading rate of a plane jet and the spreading rate of a round jet. In experiments, the spreading rate of a round jet is 15% lower than that of a plane jet, but in simulations with the standard k-ε model, the round-jet spreading rate is 15% *higher* (Wilcox, 1998).

Attempts at overcoming the round jet / plane jet anomaly have almost invariably involved modifying the closure coefficients in the dissipation-rate equation of the k-ε model. Some of these modifications (McGuirk and Rodi, 1979 and Morse, 1977) use non-local parameters, such as the half width ($r_{1/2}$), and are not applicable to general flows. The Pope (1978) modification is based on a simple physical argument and is more generally applicable. Dally, Fletcher and Masri (1998) have shown, using an elliptic flow solver, that a simple change to a closure coefficient ($C_{\varepsilon 1}$) produces more accurate and robust simulations of round and bluff-body jets than the modifications previously suggested. All of the above modifications to the standard k-ε model reduce either the generality or the numerical stability of the CFD code.

Wilcox (1988) proposed that the dissipation-rate equation of the k-ε model (Appendix Equation 6) be replaced by an equation for a specific dissipation rate defined as $\omega = k/\varepsilon$. This k-ω model predicts the behaviour of attached boundary layers in adverse pressure gradients more accurately than k-ε models, but performs poorly in free shear flows (Bardina, Huang and Coakley, 1997). The revised Wilcox (1998) turbulence model is designed to overcome the round-jet/plane-jet anomaly without degrading the simulation of boundary layer flows. In the revised model, closure coefficients which were previously constants (Wilcox, 1988) have become functions of the flow variables. Wilcox (1998) showed that the revised model works well in simulations of self-similar free-shear flows.

This paper describes the results of further testing with an unconfined turbulent jet and an elliptic flow solver. Results from the Wilcox (1998) k-ω turbulence model are compared with the experimental data of Schefer et al. (1987), with a simulation using the standard k-ε model (Launder and Sharma, 1974) and with results from a modified k-ε model.

CHOICE OF EXPERIMENTAL COMPARISON

In common with all other engineering fluid flows, important aspects of jet behaviour are governed by the boundary conditions. In cases where the boundary conditions are very strongly perturbed, as in the fluidic precessing jet (Nathan, 1988) or in an acoustically excited jet (Hill and Greene, 1977), the structure of the turbulence is very different from that found in simple turbulent jets. In the particular case of a precessing jet these differences can provide substantial benefits to gaseous flames, with a simultaneous increase in radiant heat transfer and reduction in nitric oxide emissions (Manias & Nathan, 1994; Nathan, Turns & Bandaru, 1996).

The effect of boundary conditions on jet evolution is not limited to strong perturbations. The hypothesis that the far field of a simple turbulent jet is independent of the exit plane boundary conditions is now known to be only an approximation (George, 1989). Mi, Nobes and Nathan (1999) have demonstrated that otherwise identical jets issuing from a pipe and a smooth contraction have different spreading rates and centreline scalar statistics in both the near and far-fields. Hence even apparently minor differences in boundary conditions can influence the flow significantly.

In numerical simulations, the boundary conditions must be adequately specified and physically realistic in order to obtain an acceptable solution. In order to validate a numerical simulation, it must be compared with experimental measurements. The choice of experimental comparison must be made with regard to

a) the availability of appropriate experimental data (e.g. boundary distributions of velocity and turbulence quantities),

b) the observed or deduced sensitivity of the flow to changes in boundary conditions, and

c) the feasibility of obtaining the numerical solution.

The current implementation of the Wilcox (1998) k-ω model is found to be sensitive to the choice of boundary location and boundary values of k and ω. Numerous attempts at modelling either a jet issuing into an unconfined quiescent environment or a jet emerging from a smooth contraction nozzle with a uniform velocity profile were unsuccessful in obtaining a converged solution. This means that the measurements of Panchapakesan and Lumley (1993), Wygnanski and Fiedler (1969) and Antonia and Bilger (1973) are not appropriate test cases for validation of the k-ω model. We require measurements of a jet emerging from a pipe into a co-flow, such as those provided by Schefer, Hartmann and Dibble (1987).

In Schefer's experiment a propane jet emerges from a 5 mm diameter pipe into a co-flowing air stream. The length of straight pipe upstream of the exit plane is 400 pipe diameters, thus ensuring fully developed turbulent pipe flow at the pipe exit. The centreline velocity ($U_{e,cl}$) is 70.0 m/s. A bulk flow velocity of 56.7 m/s is obtained by assuming a power law velocity distribution of the form

$$\frac{U}{U_{cl}} = \left(\frac{y}{R}\right)^{\frac{1}{n}}$$

, where n=6.69.

Upstream of the pipe exit, the co-flow air passes through a honeycomb section and then a smooth contraction to produce a mean velocity of 9.4 m/s and a turbulence intensity of 0.4%. The thickness of the external boundary layer on the pipe is 1.5 mm. It is necessary to make some minor assumptions in our simulation because Schefer omits some details, such as the wall thickness of the pipe and the temperature of the flow.

DESCRIPTION OF TURBULENCE MODELS

All of the two equation turbulence models considered below use the Boussinesq approximation to model the Reynolds stress tensor using an eddy viscosity:

$$\tau_{ij} = -\overline{u_i' u_j'} = 2\nu_T S_{ij} - \frac{2}{3} k \delta_{ij} \qquad (1)$$

Standard k-ε Model

The standard k-ε model with low-Reynolds number corrections (Launder and Sharma, 1974) is described in the Appendix (Equations 3-9). The use of low-Reynolds-number corrections allows direct comparison with the low Reynolds-number revised k-ω model.

The mean velocity, turbulence kinetic energy (k) and modelled dissipation rate (ε) are set to zero at the solid boundaries.

Modified k-ε Model

In the modified k-ε model, the closure coefficient $C_{\varepsilon 1}$=1.44 of the standard k-ε model is changed to $C_{\varepsilon 1}$=1.60. For self-similar round jets, this is equivalent to the McGuirk and Rodi (1979) and Morse (1977) modifications to the dissipation rate equation of the standard k-ε model.

Revised Wilcox (1998) k-ω Model

The equations for the revised k-ω turbulence model, which is a low-Reynolds-number model, are given in the Appendix (Equations 10-15).

At the solid boundaries, mean velocity and turbulence kinetic energy are zero. For the viscous sublayer at a solid boundary, Wilcox (1998) provides the solution

$$\lim_{y \to 0} \omega y^2 = -\frac{6\nu}{\beta_0} . \qquad (2)$$

Wilcox attributes the success of the k-ω model in modelling adverse pressure gradient boundary layers to the lack of cross-diffusion

$$\chi_k \equiv \frac{1}{\omega^3} \frac{\partial k}{\partial x_j} \frac{\partial \omega}{\partial x_j}$$

in the ω equation and a corresponding absence of cross-diffusion in the modelled boundary layer. On the other hand, changing the dependent variables from ε to ω in Equation 5 shows that cross-diffusion is an implicit feature of the k-ε model. Apart from the differences in the closure coefficients this is the major difference between the two models.

The lack of a cross diffusion term in the ω equation is also believed to be responsible for the poor performance of the 1988 k-ω model in free shear flows. In his 1998 model, Wilcox uses the cross diffusion parameter, which is large in free shear flows and small in boundary layers, to selectively increase the dissipation term in the k equation and hence to reduce the eddy viscosity in free shear flows.

Pope (1978) suggested a vortex stretching modification to the ε equation in the k-ε model. He argued that in areas of the flow where mean vorticity is stretched, there is a reduction in length scale, and so it is likely in these areas that turbulence vorticity is also stretched and reduced in scale. A reduction in turbulence scale implies an increase in dissipation. If the destruction term in the dissipation equation ($C_{\varepsilon 2}$) is reduced in proportion to the mean vortex stretching, net dissipation is increased. This reduces the eddy viscosity, and so decreases the spreading rate.

Wilcox (1998) introduces essentially the same argument in his ω equation, but his adjustment is bounded (Equation 13) rather than proportionate (Pope, 1978). The Pope (1978) correction to the standard k-ε model is not considered here because it reduces the convergence rate of the calculation significantly (Dally et al. 1998).

The revised Wilcox (1998) model was implemented in the commercial CFD code CFX 4.2 (CFX, 1998). User-defined subroutines were written to calculate the closure coefficients as functions of the flow variables, to overwrite the existing eddy viscosity and to overwrite the production and dissipation terms in the existing k-ω implementation.

PROCEDURE

For the jet-flow the computational domain is an axisymmetric grid extending 50 pipe diameters downstream from the pipe exit, 80 pipe diameters upstream from the pipe exit and 20 pipe diameters from the axis. The 80 pipe diameters of development length make it possible to establish a fully developed turbulent pipe flow at the pipe exit. Within the pipe, the axisymmetric grid has 20 cells in the radial direction and 60 cells in the axial direction. The overall number of cells in the axial and radial directions is 140 and 60, respectively. As the grid approaches the walls its spacing is reduced in order to resolve the viscous sublayer. All cells adjacent to the walls are within $0 \leq y^+ < 1.7$. The axial and radial grid spacing becomes larger with increasing downstream distance from the pipe exit.

Flow variables are uniform at the inlet boundaries, and zero pressure is specified at the remaining external boundaries. Van Leer differencing is used for the convection term in the scalar transport equations (k, ε, mass fraction and enthalpy), and QUICK is used for the velocity equations. The calculation is continued until the ratio of mass residuals to mass entering the pipe is less than 0.5×10^{-6}.

RESULTS

In Figure 1, the velocity distribution of the fully developed pipe flow is compared with the experimental results of Laufer (1952) for a pipe Reynolds number of 50,000. All three turbulence models produce a fully developed flow at distances more than 55 diameters from the pipe inlet. The velocity distributions for the k-ω model and the standard k-ε model are in very close agreement. Both agree reasonably with experimental data. The velocity distribution from the modified k-ε model matches the experimental data less closely. All three models are considered to provide a useful pipe exit boundary condition for the jet flow simulation.

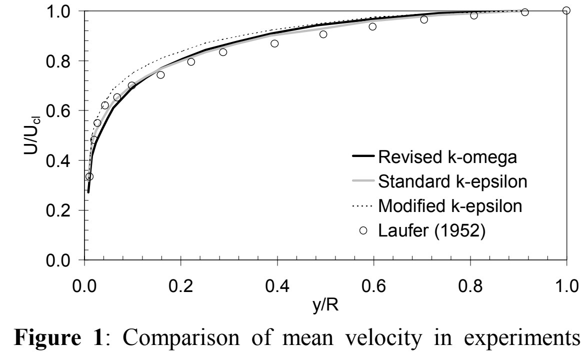

Figure 1: Comparison of mean velocity in experiments and simulations of fully developed pipe flow.

In Figure 2, nondimensional centreline mean velocity is plotted as a function of nondimensional distance from the pipe exit. In the turbulent far field ($x/D_j > 20$), centreline velocity from the standard k-ε model decays about 20% faster than the experimental data. This finding is consistent with previous investigations (eg. Wilcox, 1998). In contrast, centreline velocity from the modified k-ε model and revised k-ω model decays more slowly than the experimental data, by about 14% and 11% respectively. The modified k-ε model and the revised k-ω model predict similar centreline velocity decay. Results in the near field ($x/D_j < 5$) are dominated by the velocity distribution of the fully developed pipe flow.

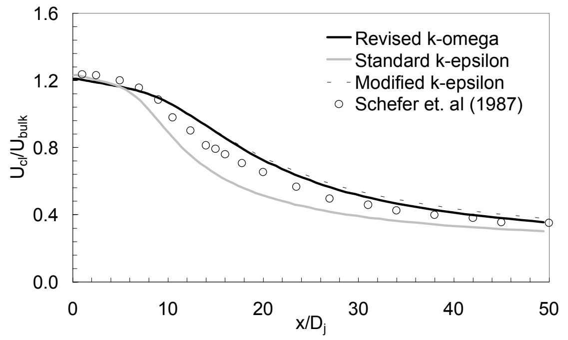

Figure 2: Comparison of the centreline axial mean velocity in experiments and simulations of a round jet in co-flow.

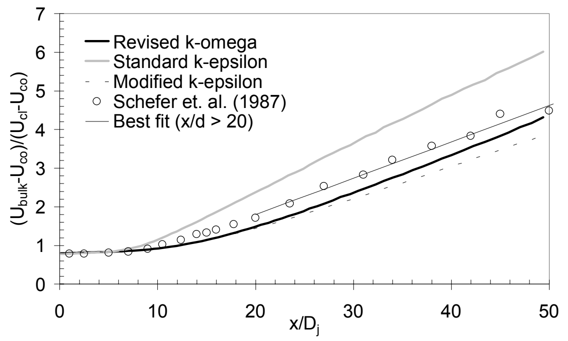

Figure 3: Comparison of the centreline axial mean velocity in experiments and simulations of a round jet in co-flow.

Figure 3 shows that, in the turbulent far field of the jet, the reciprocal of the jet centreline velocity excess

$$\frac{U_{bulk} - U_{co}}{U_{cl} - U_{co}}$$

becomes a linear function of the distance from the pipe exit, although the linear coefficient is different in every case.

Radial distributions of velocity at a distance $x=30D_j$ from the pipe exit are shown in Figure 4. In Figure 4(a) the radius is nondimensionalised by distance from the virtual origin and therefore indicates differences in the spreading rates to be seen. The half width ($r_{1/2}$) spreading rate for the present jet in a coflow is significantly smaller than that of an unconfined jet (Table 1).

In Figure 4(b), the radial distribution of mean velocity in the "self similar" region of the jet is normalised with local velocity and length scales. The shape of the velocity distribution is therefore expected to be less dependent of the jet spreading rate, and more dependent on distribution of the mixing length scale or, for the experimental data, on the mechanisms of turbulent motion. As in simulations of self-similar jets (Wilcox, 1998), differences between the simulations and the experimental data are most apparent near the edge of the jet, where the real flow is intermittently turbulent and "laminar".

	Jet Spreading Rate	
	U_{co}/U_{cl} = 0.134	U_{co}/U_{cl} = 0.0 (no co-flow)
Expt.	0.061 (Schefer)	0.086-0.096 (Wygnanski & Fiedler, 1969; Panchapakesan & Lumley, 1993)
Std. k-ε	0.068 (present)	0.120 (Wilcox, 1998)
Mod. k-ε	0.043 (present)	-
1998 k-ω	0.052 (present)	0.088 (Wilcox, 1998)

Table 1: A comparison of measured and predicted half width ($r_{1/2}$) spreading rates of jets with and without a coflow.

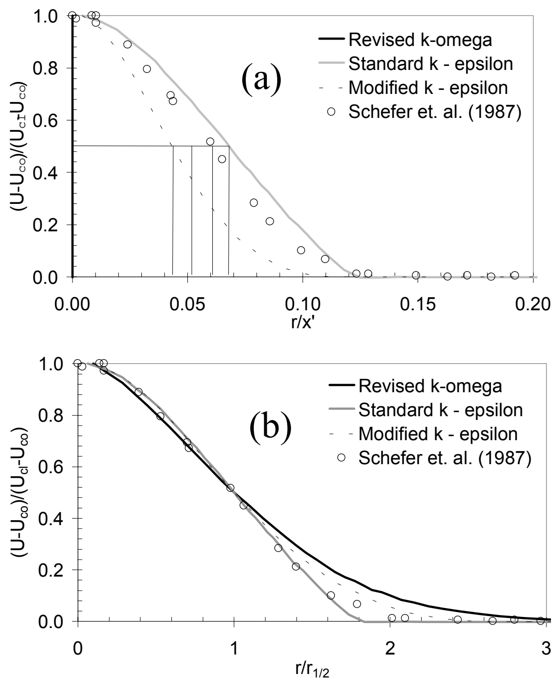

Figure 4: Radial distributions of velocity obtained at an axial distance of 30 D_j in experiments and simulations of a round jet in co-flow; (a) variation in spreading rates; (b) variation in shape.

It is clear from Figure 5 that none of the turbulence models tested here are able to provide an accurate prediction of turbulence kinetic energy. Even in the "best" simulation, which is provided by the k-ω model, the peak turbulence kinetic energy is twice the experimental value. The turbulence kinetic energy is estimated from the experimental data with

$$k = \frac{1}{2}\left(\overline{u'^2} + 2\overline{v'^2}\right)$$

because the third component of fluctuating velocity (w') was not measured.

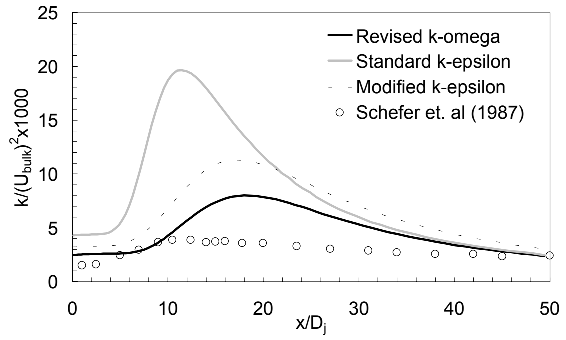

Figure 5: Comparison of the centreline turbulence kinetic energy in experiments and simulations of a round jet in co-flow.

DISCUSSION

The results from the revised k-ω model are generally encouraging. In a pipe flow it provides a level of accuracy similar to that of the standard k-ε model, and in a round jet it is about as accurate as the modified k-ε model, but its closure coefficients do not need to be changed to suit the flow.

Wilcox (1998) has performed calculations in self-similar jet flow using a numerical method that solves the self-similar equations. He used a transformed radial coordinate that maps the edge of the shear layer to infinity. This removes the need to compute values outside the shear layer and has the effect of clustering grid points near the edge of the jet. The self-similar simulation requires no pipe exit boundary conditions.

Wilcox obtained a radial distribution of velocity and spreading rate that agree well with the experimental data of Wygnanski and Fiedler (1969). However, the agreement between the k-ω model and the experimental data in the present case in which inlet boundaries and a co-flow are present is not quite as good (Table 1).

One feature of Schefer's experiment not included in our numerical simulations is a smooth contraction in the duct providing the co-flow. As a result the thickness of the simulated boundary layer on the outside of the pipe at the exit (δ=0.75D_j) is more than twice the value measured in the experiments (δ=0.3D_j). Another possible difference between the experiment and our simulations arises because the temperature, and hence the density, of the propane jet used in the experiments was not reported. It has been assumed to be 20^{o}C in the calculations.

The current implementation of the revised (1998) k-ω model can produce anomalous and extremely rapid decay of the jet, especially when the development length of boundary layers upstream of the pipe exit is very short. Low turbulence intensities at the upstream boundaries in either the jet or co-flow, and low co-flow velocities tend to exacerbate this problem. The anomaly is avoided by allowing the pipe flow and the co-flow upstream of the pipe exit to develop over a length of 80 pipe diameters. This behaviour may be related to the reported sensitivity to boundary conditions (Menter, 1992).

The simulations in this paper use low-Reynolds number turbulence models, which must be integrated through the viscous sublayer. In the future, the use of wall functions (Wilcox, 1998) may speed up the calculations.

SUMMARY

The revised k-ω turbulence model is implemented in a commercial CFD package and it is used to simulate a round jet in a co-flow. It performs at least as well as the modified k-ε model and better than the standard k-ε model. The errors in the calculated mean velocity are in the order of 10%. The ability to calculate both boundary layer and free-shear flows without explicitly adjusting the closure coefficients is a significant advantage which justifies further development of the model.

The issue of sensitivity to boundary conditions requires further investigation.

ACKNOWLEGMENTS

Mr. R. C. Morgans acknowledges the financial support of the Turbulence Energy and Combustion group in the Departments of Mechanical Engineering and Chemical Engineering at the University of Adelaide.

The valuable help of Dr. J. Mi and Mr. B. M. Ghazali is also gratefully acknowledged.

REFERENCES

ANTONIA, R. A. and BILGER, R. W. (1973) "An experimental investigation of an axisymmetric jet in a co-flowing air stream", *Journal of Fluid Mechanics*, **61**, 805-822.

BARDINA, J. E., HUANG, P. G. and COAKLEY, T. J. (1997), "Turbulence Modeling Validation, Testing, and Development", *NASA-TM-110446*.

CFX (1998), "CFX flow solver manual", AEA Technology, Harwell Laboratory, Didcot, Oxon, UK

DALLY, B. B., FLETCHER, D. F. and MASRI, A. R. (1998) "Flow and mixing fields of turbulent bluff-body jets and flames", *Combust. Theory Modelling*, **2**, 193-219.

GEORGE, W.K. (1989) "The self preservation of turbulent flows and its relation to initial conditions and coherent structures", *Recent Advances in Turbulence*, Editors R.E.A Arndt and W.K. George, Hemisphere, New York, 39-73

HILL, W. G. JR. and GREENE P. R., (1977) "Increased turbulent jet mixing rates obtained by self-excited acoustic oscillations", *Journal of Fluids Engineering, Transactions of the ASME*, **99**, 520-525.

LAUNDER, B. E. and SHARMA, B.I. (1974), "Application of the energy dissipation model of turbulence to the calculation of flow near a spinning disk", *Letters in Heat and Mass Transfer*, Vol. 1 No. 2, 131-138

LAUFER, J. (1952), "The structure of turbulence in fully developed pipe flow", *NACA Report 1174*.

MANIAS, C. G. and NATHAN, G. J. (1994) "Low NO_x clinker production", *World Cement*, **25**, 54-56.

McGUIRK, J. J. and RODI, W. (1979), "The calculation of three-dimensional turbulent free jets", *1st Symp. On Turbulent Shear Flows*, ed. DURST, F., LAUNDER, B. E., SCHMIDT, F. W. and WHITELAW, J. W., 71-83

MENTER, F. R. (1992), "Influence of freestream values on k-ω turbulence model predictions", *AIAA J.* **30**, 1657-1659.

MI, J., NOBES, D. S. and NATHAN, G. J. (1999), "Influence of jet exit conditions on the passive scalar field of an axisymmetric free jet", *Submitted to the Journal of Fluid Mechanics.*

MORSE, A. P. (1977), "Axisymmetric turbulent shear flows with and without swirl", *PhD Thesis*, London University.

NATHAN, G. J. (1988), "The enhanced mixing burner", *PhD Thesis*, Dept. Mech, Eng., The University of Adelaide.

NATHAN, G. J., TURNS, S. R. and BANDARU, R. V. (1996) "The influence of jet precession on NO_x emissions and radiation from turbulent flames", *Comb. Sci. Tech.,* **112**, 211-230.

PANCHAPAKESAN, N. R. and LUMLEY, J. L. (1993), "Turbulence measurements in axisymmetric jets of air and helium. Part 1. Air jet", *Journal of Fluid Mechanics*, **246**, 197-233.

POPE, S. B. (1978), "An explanation of the round-jet/plane-jet anomaly", *AIAA J.* **16** 279-281.

SCHEFER, R. W., HARTMANN, V. and DIBBLE, R. W. (1987) "Conditional Sampling of Velocity in a Turbulent Nonpremixed Propane Jet", *Sandia National Laboratories Report SAND87-8610.*

WILCOX, D. C., (1988) "Reassessment of the scale-determining equation for advanced turbulence models", *AIAA Journal*, **26**, 1299-1310.

WILCOX, D. C., (1998) "Turbulence Modeling for CFD", DCW Industries, La Cañada, California.

WYGNANSKI, I. and FIEDLER, H. (1969) "Some measurements in the self-preserving jet", *Journal of Fluid Mechanics*, **38**, 557-612.

APPENDIX – TURBULENCE MODEL EQUATIONS

Standard k-ε Model

$$\frac{\partial k}{\partial t}+U_j\frac{\partial k}{\partial x_j}=\tau_{ij}\frac{\partial U_i}{\partial x_j}-\varepsilon-D+\frac{\partial}{\partial x_j}\left[\left(\nu+\frac{\nu_T}{\sigma_k}\right)\frac{\partial k}{\partial x_j}\right] \tag{3}$$

$$\frac{\partial \varepsilon}{\partial t}+U_j\frac{\partial \varepsilon}{\partial x_j}=C_{\varepsilon 1}\frac{\varepsilon}{k}\tau_{ij}\frac{\partial U_i}{\partial x_j}-C_{\varepsilon 2}f_2\frac{\varepsilon}{k}\varepsilon+E+\frac{\partial}{\partial x_j}\left[\left(\nu+\frac{\nu_T}{\sigma_\varepsilon}\right)\frac{\partial k}{\partial x_j}\right] \tag{4}$$

$$\nu_T=C_\mu f_\mu\frac{k^2}{\varepsilon} \tag{5}$$

$$f_\mu=\exp\left(\frac{-3.4}{\left(1+\frac{R_T}{50}\right)^2}\right),\ f_2=1-0.3\exp\left(-R_T^2\right) \tag{6}$$

$$D=2\mu\left(\frac{\partial k^{\frac{1}{2}}}{\partial x_i}\right)^2,\ E=2\mu\nu_T\left(\frac{\partial^2 U}{\partial x_i\partial x_i}\right)^2 \tag{7}$$

$$R_T=\frac{k^2}{\nu\varepsilon} \tag{8}$$

$$C_\mu=0.09\,,\ C_{\varepsilon 1}=1.44\,,\ C_{\varepsilon 2}=1.92\,,\quad \sigma_k=1.0\,,\ \sigma_\varepsilon=1.3 \tag{9}$$

Revised Wilcox (1998) k-ω Model

$$\frac{\partial k}{\partial t}+U_j\frac{\partial k}{\partial x_j}=\tau_{ij}\frac{\partial U_i}{\partial x_j}-\beta^*k\omega+\frac{\partial}{\partial x_j}\left[\left(\nu+\sigma^*\nu_T\right)\frac{\partial k}{\partial x_j}\right] \tag{10}$$

$$\frac{\partial \omega}{\partial t}+U_j\frac{\partial \omega}{\partial x_j}=\alpha\frac{\omega}{k}\tau_{ij}\frac{\partial U_i}{\partial x_j}-\beta\omega^2+\frac{\partial}{\partial x_j}\left[\left(\nu+\sigma\nu_T\right)\frac{\partial k}{\partial x_j}\right] \tag{11}$$

$$\nu_T=\frac{k}{\omega},\ \beta^*=\beta_0^*f_\beta,\ \beta=\beta_0 f_\beta \tag{12}$$

$$f_\beta=\frac{1+70\chi_\omega}{1+80\chi_\omega},\ \chi_\omega\equiv\left|\frac{\Omega_{ij}\Omega_{jk}S_{ki}}{\left(\beta_0^*\omega\right)^3}\right| \tag{13}$$

$$f_{\beta^*}=\begin{cases}1, & \chi_k\le 0\\ \dfrac{1+680\chi_k^2}{1+400\chi_k^2}, & \chi_k\ge 0\end{cases},\ \chi_k\equiv\frac{1}{\omega^3}\frac{\partial k}{\partial x_j}\frac{\partial \omega}{\partial x_j} \tag{14}$$

$$\alpha=0.52\,,\ \beta_0^*=0.09\,,\ \beta_0=0.072\,,\quad \sigma^*=0.5\,,\ \sigma=0.5 \tag{15}$$